Synthesis and characterization of electroactive hyperbranched aromatic polyamides based on A_2B-type triphenylamine moieties†

Guey-Sheng Liou,* Hung-Yi Lin and Hung-Ju Yen

Received 21st May 2009, Accepted 6th August 2009
First published as an Advance Article on the web 27th August 2009
DOI: 10.1039/b910081d

A series of electrochromic aromatic hyperbranched polyamides with electroactive triphenylamine (TPA) units were prepared from the phosphorylation polyamidation reactions of a newly A_2B type monomer, 4-amino-4′,4″-dicarboxytiphenylamine, with AB monomer and end-capping agent, respectively. These polymers were readily soluble in many organic solvents and showed useful levels of thermal stability associated with high glass-transition temperatures (201–221 °C) and high char yields (higher than 71% at 800 °C in nitrogen). The polymer films showed reversible electrochemical oxidation with a high contrast ratio in the visible region, and exhibited high coloration efficiency (CE), and high-level stability for an electrochromic operation. The polyamide **P2** thin film revealed high coloration efficiency (CE = 426 cm^2/C) and optical transmittance change ($\Delta\%T = 79\%$) in the visible region with reversible electroactive stability (over 1000 times within 5% loss).

Introduction

Recently, dendritic macromolecules, such as dendrons, dendrimers and hyperbranched polymers have received considerable attention due to their unique structures, chemical and physical properties.[1] They are mainly classified into dendrimers with well-defined structures and hyperbranched polymers having statistically branched architecture. Hyperbranched polymers resemble dendrimers in many physical properties such as low viscosity, high solubility, and lack of significant entanglement in the solid state. In contrast, hyperbranched polymers are readily synthesized by one-step polymerization of AB_n monomers. This is advantageous over the multistep synthesis of dendrimers because of the rapid production of large quantities.[2] Furthermore, various functional groups can be introduced into hyperbranched polymers and the properties can be tuned by the chemical modification of end functional groups. A wide variety of hyperbranched polymers such as polyesters,[3] polyethers,[4] polyphenylenes,[5] poly(ether ketone)s[6] and polyamides[7] have been reported in the literatures. In addition, the incorporation of triphenylamine (TPA) groups into hyperbranched polyamine, poly(3,4-ethylenedioxythiophene- didodecyloxybenzene), polyfluorene, polyphenylene, polyphenylenevinylene, and polythiophene backbones were also investigated and utilized for applications, such as solar cells[8] and light-emitting[9] materials. However, there were just a few spectroelectochemical studies[10] of TPA-based hyperbranched polymers and no electrochromic results reported to date from hyperbranched aromatic polyamide with TPA backbone structures.

Photochromism is a reversible photoinduced transformation of a molecule between two isomers exhibiting different absorption spectra. This phenomenon is of great interest for emerging technologies, such as optical data storage and optical switching for optoelectronic devices.[11] Electrochromic materials exhibit a reversible optical change in absorption or transmittance upon electrochemically oxidized or reduced, such as transition-metal oxides, inorganic coordination complexes, organic molecules, and conjugated polymers.[12] The investigation of electrochromic materials has been directed towards optical changes in the visible region (*e.g.*, 400–800 nm) because the color changes are more conveniently controlled and tuned by just adjusting the applied potential, therefore, electrochromic polymers are especially useful for antiglare back-mirrors, tunable windows, and electrochromic displays.

Wholly aromatic polyamides can be readily synthesized by direct polycondensation of diacids and diamines in the presence of condensing agents such as triphenyl phosphite and pyridine.[13] They are characterized as highly thermally stable polymers with a favorable balance of physical and chemical properties. However, the rigidity of the backbone and strong hydrogen bonding result in high melting or glass-transition temperatures and limit solubility in most organic solvents.[14] These properties make them generally intractable or difficult to process, thus restricting their applications. Fortunately, hyperbranched aromatic polyamides are soluble in polar aprotic organic solvents, and even in tetrahydrofuran (THF).[15]

In 1952, Flory reported a one-step polymerization of AB_2 type monomers and copolymerization of AB and AB_2 type monomers.[16] Then, some reports showed a "AB_2 + AB" approach about copolymers of AB and AB_2 type monomers.[17] The introduction of the AB monomer allows to control the content of branching units. Therefore, our strategy was to synthesize the A_2B-type monomer with the electroactive TPA moiety. In addition to the high solubility of the resulting A_2B-type

Functional Polymeric Materials Laboratory, Institute of Polymer Science and Engineering, National Taiwan University, No.1, Sec. 4, Roosevelt Rd., Taipei, 10617, Taiwan. E-mail: gsliou@ntu.edu.tw

† Electronic supplementary information (ESI) available: Monomer synthesis, table of thermal and optical properties, IR spectra of monomers and polyamides, ^1H and ^{13}C NMR spectra of monomers, GPC curves of hyperbranched polyamides, TGA and TMA curves of hyperbranched polyamide **P3**, UV-visible transmission spectra of polyamide films, cyclic voltammetric diagrams of polyamide **P2**, calculation of optical switching time of polyamide **P2** film. See DOI: 10.1039/b910081d

hyperbranched polyamide, the chemical modification of end functional groups by incorporating *para*-methoxy-substituted TPA groups could lower the oxidation potentials and afford different electrochromic characteristics.[18] Furthermore, the content of branching units could also be tuned by copolymerization of the A_2B and AB-type monomers. Because of the incorporation of packing-disruptive TPA units along the polymer backbone, all of the polymers exhibited good solubility in polar organic solvents. The transparent and amorphous thin films could be prepared by spin-coating and inkjet-printing techniques that are beneficial for their fabrication of large-area thin-film optoelectronic devices.

The TPA-based novel A_2B-type monomer, 4-amino-4′,4″-dicarboxytiphenylamine (**3**), was therefore synthesized in this contribution, then a series of electrochromic aromatic hyperbranched polyamides could be prepared by phosphorylation polyamidation reactions of the newly A_2B-type monomer with AB monomer and end-capping agent, respectively. The general properties such as inherent viscosities, molecular weights, solubility, and thermal properties are described. The electrochemical, electrochromic, and photophysical properties of these polymers are also investigated.

Experimental

Materials

4-Amino-4′,4″-dimethoxytriphenylamine[18b] (**B-OMe$_2$**) (mp: 133–134 °C) and 4-amino-4′-carboxy-4″-methoxytiphenylamine[19] (**AB-OMe**) (mp: 256–258 °C) were synthesized according to a previously reported procedure. Tetrabutylammonium perchlorate (TBAP) (ACROS) was recrystallized twice from ethyl acetate under a nitrogen atmosphere and then dried *in vacuo* prior to use. All other reagents were used as received from commercial sources.

Polymer synthesis

The synthesis of polyamides **P1–P3** was shown as following the synthetic route. **P1**: a mixture of 0.52 g (1.5 mmol) of 4-amino-4′,4″-dicarboxytiphenylamine (**3**), 0.18 g of calcium chloride ($CaCl_2$), 1.2 mL of triphenyl phosphate (TPP), 0.6 mL of pyridine, and 1.0 mL of *N*-methyl-2-pyrrolidinone (NMP) was heated with stirring at 70 °C for 3 h. **P2**: 0.35 g (1.0 mmol) of monomer **3**, 0.12 g of $CaCl_2$, 0.8 mL of TPP, 0.4 mL of pyridine, and 1.0 mL of NMP was heated with stirring at 70 °C for 1.5 h, followed by adding 0.32 g (1.0 mmol) of 4-amino-4′,4″-dimethoxytriphenylamine (**B-OMe$_2$**) and heated with stirring at 105 °C for 3 h. **P3**: 0.35 g (1.0 mmol) of monomer **3**, 0.33 g (1.0 mmole) of 4-amino-4′-carboxy-4″-methoxytiphenylamine (**AB-OMe**), 0.12 g of $CaCl_2$, 0.8 mL of TPP, 0.4 mL of pyridine, and 1.0 mL of NMP was heated with stirring at 70 °C for 3 h. Then, the obtained polymer solutions were poured slowly into 150 mL of stirred methanol giving rise to the precipitate that was collected by filtration, washed thoroughly with hot water and methanol, and dried at 100 °C. The yields of **P1–P3** were 0.40 g (81%), 0.61 g (94%), and 0.58 g (93%), respectively. Finally, reprecipitation from *N,N*-dimethylacetamide (DMAc) into methanol was carried out twice for further purification.

Preparation of the film

A solution of the polymer was made by dissolving about 0.55 g of the hyperbranched aromatic polyamide sample in 8.0 mL of DMAc. The homogeneous solution was poured into a 9-cm glass Petri dish, which was placed in a 90 °C oven for 3 h to remove most of the solvent; then the semidried film was further dried *in vacuo* at 170 °C for 7 h. The obtained films were used for solubility tests and thermal analyses.

Results and discussion

Monomer synthesis

The synthesis procedure of A_2B monomer and two intermediate compounds was outlined in Scheme 1. 4,4′-Dicyano-4″-nitrotriphenylamine **1** was synthesized from the nitroaniline and 4-fluorobenzonitrile by a nucleophilic substitution reaction, and 4,4′-dicarboxy-4″-nitrotriphenylamine **2** could be readily prepared by hydrolysis of compound **1** in an alkaline solution. A new A_2B monomer **3**, 4-amino-4′,4″-dicarboxytiphenylamine, was synthesized by hydrogen Pd/C-catalyzed reduction of the compound **2** and shown in Scheme 1. Elemental analysis, IR, and ^{1}H and ^{13}C NMR spectroscopic techniques were used to identify the structures of the intermediate compound **1**, **2**, and A_2B monomer **3**. The FT-IR spectra of the synthesized compounds **1–3** are illustrated in Fig. S1.† The dinitrile compound **1** showed a cyano characteristic band at 2219 cm^{-1} (–C≡N stretch) and two characteristic bands at 1582, 1323 cm^{-1} (–NO_2 stretch), respectively. After hydrolysis and reduction, the characteristic absorptions of the cyano and nitro group disappeared, and the primary amino group showed the typical absorption pair at 3450 and 3365 cm^{-1} with C=O and O–H stretching absorptions at 1686 and 2700–3600 cm^{-1}, respectively. Fig. S2 and S3 illustrate the ^{1}H NMR and ^{13}C NMR spectra of the compounds **1–3**, respectively. The ^{13}C NMR spectra of compound **2** confirm that the cyano group was completely converted into the carboxylic acid group by the appearance of a carbonyl carbon peak at 166.85 ppm instead of cyano carbon at 118.80 ppm. Other important evidence is the shifting of the carbon resonance signal of C^2 adjacent to the cyano or carboxyl group. The C^2 of compound **1** resonated at a higher field (107.25 ppm) than the other aromatic carbons because of the anisotropic shielding by the electron of the cyano group. After hydrolysis, the resonance peak of C^2 shifted to a lower field (127.45 ppm) because of the lack of anisotropic shielding. In ^{1}H NMR spectra of compound **2**, a broad characteristic peak around 12–13 ppm (–COOH) proved that the cyano groups were converted into the carboxylic acid groups. Besides, the shifting of H_d from 8.14 to 6.61 ppm could be used to judge the successful reduction of A_2B monomer **3**.

Polymer synthesis

According to the phosphorylation technique described by Yamazaki,[13] the hyperbranched aromatic polyamide homopolymer **P1** and the copolymer **P3** were prepared by direct polycondensation of A_2B monomer **3** and copolymerization of A_2B monomer **3** and AB monomer **AB-OMe** in the presence of triphenyl phosphite and pyridine as condensation agents. The hyperbranched polymer **P2** was synthesized by the reaction of

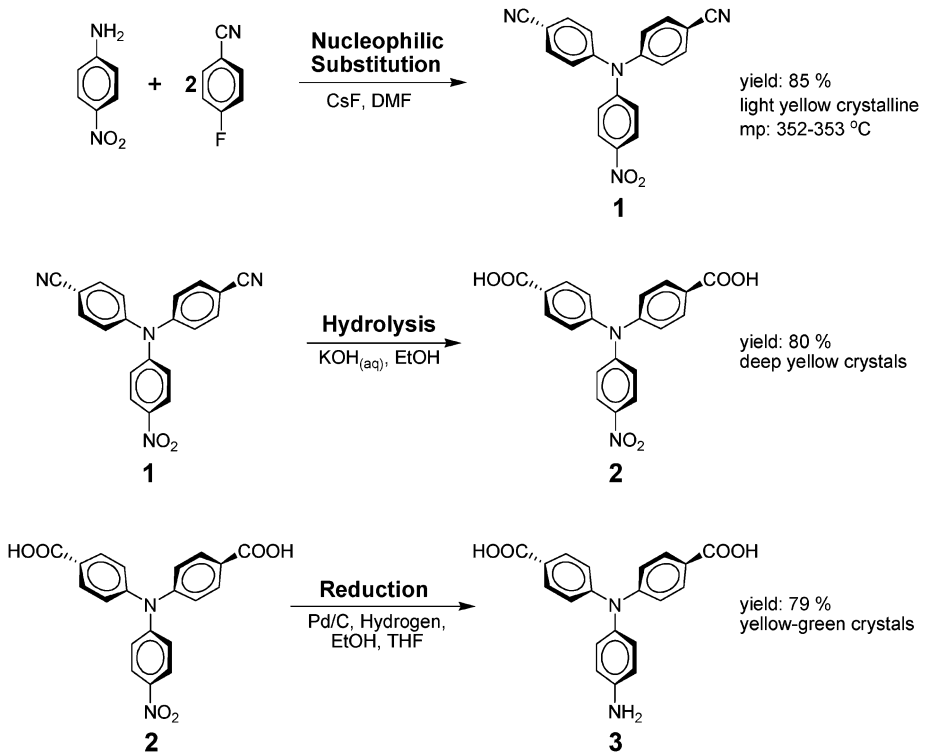

Scheme 1 Synthetic route to A_2B monomer.

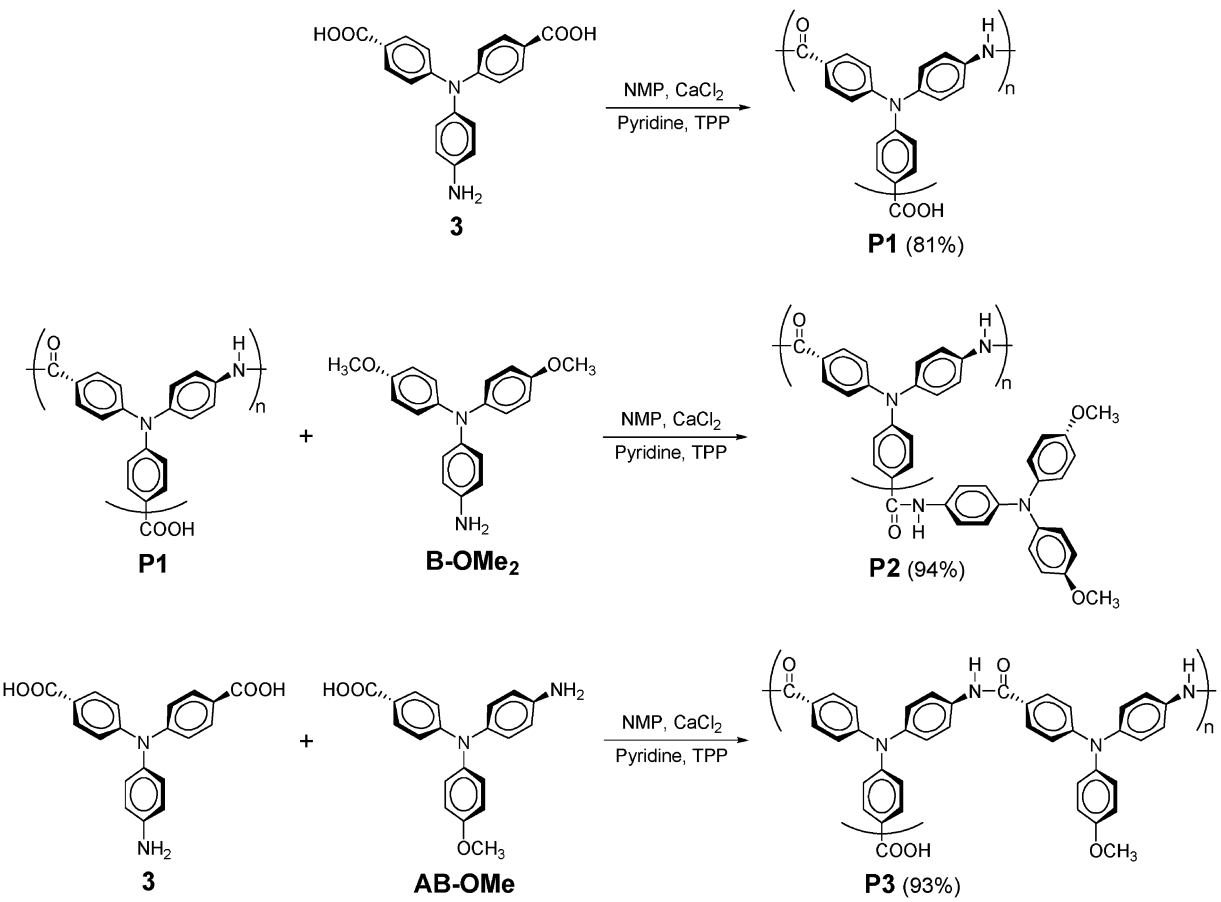

Scheme 2 Synthesis of hyperbranched polyamides.

Table 1 Inherent viscosity, molecular weights, and solubility of polyamides

Code	η_{inh}[a]/dL g^{-1}	M_w[b]	M_n	PDI[c]	Solubility in various solvents[d]					
					NMP	DMAc	DMF	THF	$CHCl_3$	CH_3CN
P1	0.19	13300	6500	2.05	++	++	++	++	—	—
P2	0.24	42600	28300	1.51	++	++	++	++	—	—
P3	0.22	34400	20600	1.67	++	++	++	++	—	—

[a] Measured at a polymer concentration of 0.5 g dL^{-1} in NMP at 30 °C. [b] Average molecular weights relative to polystyrene standard in NMP by GPC. [c] Polydispersity Index = M_w/M_n. [d] The solubility was determined with a 1 mg sample in 1 mL of a solvent. ++, soluble at room temperature; –, insoluble even on heating. $CHCl_3$: chloroform.

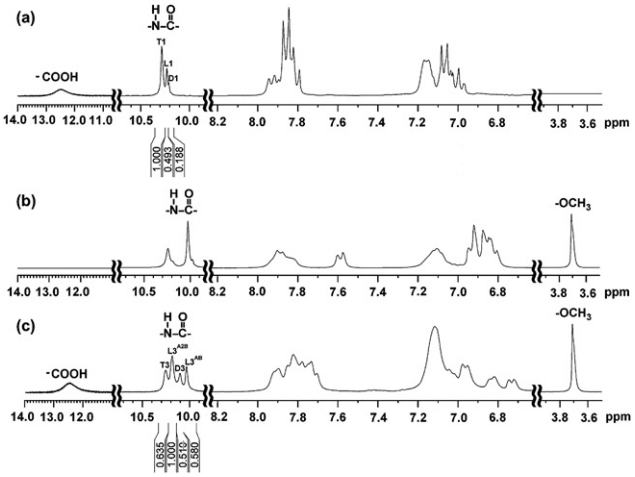

Fig. 1 ^{1}H NMR spectra of (a) **P1**, (b) **P2**, and (c) **P3**.

polymer **P1** with amino monomer **B-OMe$_2$** as the end-capping agent as shown in Scheme 2. The obtained polyamides had inherent viscosities in the range of 0.19–0.24 dL g^{-1} with weight-average molecular weights (M_w) and polydispersity index (PDI) in the range of 13300–42600 Da and 1.51–2.05, respectively, relative to polystyrene standards (Table 1). The GPC curves of **P1–P3** were shown in Fig. S4.† The formation of polyamides was also confirmed by IR and NMR spectroscopy. Fig. S5† shows IR spectra for **P1–P3**, and the typical polyamide **P1** exhibited broad bands around 3650–3100 cm^{-1} (–OH stretch) and 1686 cm^{-1} (amide carbonyl stretch). After the end-capping reaction with **B-OMe$_2$**, polyamide **P2** showed the characteristic amide bands around 3311 (–NH stretch) and 1670 cm^{-1} (amide carbonyl stretch) but the absorption of carboxylic acid group disappeared. Typical ^{1}H NMR spectra of **P1–P3** in DMSO-d_6 were shown in Fig. 1. The multiple peaks around 10.0 ppm were attributed to the amide groups formed during polymerization. The carboxylic acid group around 13 ppm was not observed for **P2**, indicating that the reaction between the carboxylic acid groups on homo-polymer **P1** and end-capping agent **B-OMe$_2$** was complete.

Degree of branching (DB)

TPA-based hyperbranched polymers from A_2B type monomer were composed of linear (**L**), dendritic (**D**), and terminal (**T**) units as shown in Scheme 3. The DB for hyperbranched polymers has been described as the ratio of the sum of **D** and **T** units *versus* the total units (**L**, **D**, and **T** units),[3a] and is generally calculated according to the following equation: DB = **(D + T)/(D + T + L)**. In the proton NMR spectra (Fig. 1), polyamide **P1** showed three kinds of amide (–NH) peaks which can be attributed to dendritic (**D1**), linear (**L1**), and terminal (**T1**) units, respectively. DB of **P1** and **P3** were calculated as 0.71 and 0.42, respectively, based on the integral intensity of quantitative ^{1}H NMR data. The unusually high DB value of **P1** might be because the terminal strong electron withdrawing group, 4-amido-4′,4″-di(carboxylic acid)TPA, increased the reactivity of the nearby acid group, thus increasing the number of dendritic units (as shown in Scheme 4). The lower DB of **P3** was attributed to the copolymerization of A_2B monomer **3** with AB monomer **AB-OMe** which increased the **L** unit as well as decreased the branching units.

Basic characterization

The solubility properties of the hyperbranched polyamides **P1–P3** were investigated qualitatively, and the results are also listed in Table 1. Most of the polyamides are readily soluble in polar aprotic organic solvents such as NMP, DMAc, *N,N*-dimethylformamide (DMF), dimethyl sulfoxide (DMSO), and tetrahydrofuran (THF). Thus, the excellent solubility makes these polymers potential candidates for practical applications by spin-coating or inkjet-printing processes to afford high performance thin films for optoelectronic devices. Their high solubility and amorphous properties can be attributed to the incorporation of bulky, three-dimensional TPA moiety along the polymer backbone, which results in a high steric hindrance for close packing, and thus reduces their crystallization tendency.

The thermal properties of polyamides were examined by TGA, TMA and DSC, and the thermal behavior data are summarized in Table S1.† Typical TGA and TMA curves of polyamide **P3** are shown in Fig. S6.† All the prepared polyamides exhibited good thermal stability with insignificant weight loss up to 500 °C under nitrogen or air atmosphere. The 10% weight loss temperatures of these polymers in nitrogen and air were recorded in the range of 505–550 and 510–535 °C, respectively. The concentration of carbonized residue (char yield) of these polymers in a nitrogen atmosphere was more than 71% at 800 °C. The high char yields of these polymers can be ascribed to their high aromatic content. The glass-transition temperatures (T_g) of polyamides **P1–P3** could be easily measured by the DSC thermograms; they were observed in the range of 193–211 °C, depending upon the stiffness of the polymer chain. All the polymers indicated no clear melting endotherms up to the decomposition temperatures on the DSC thermograms, which supports the amorphous nature of

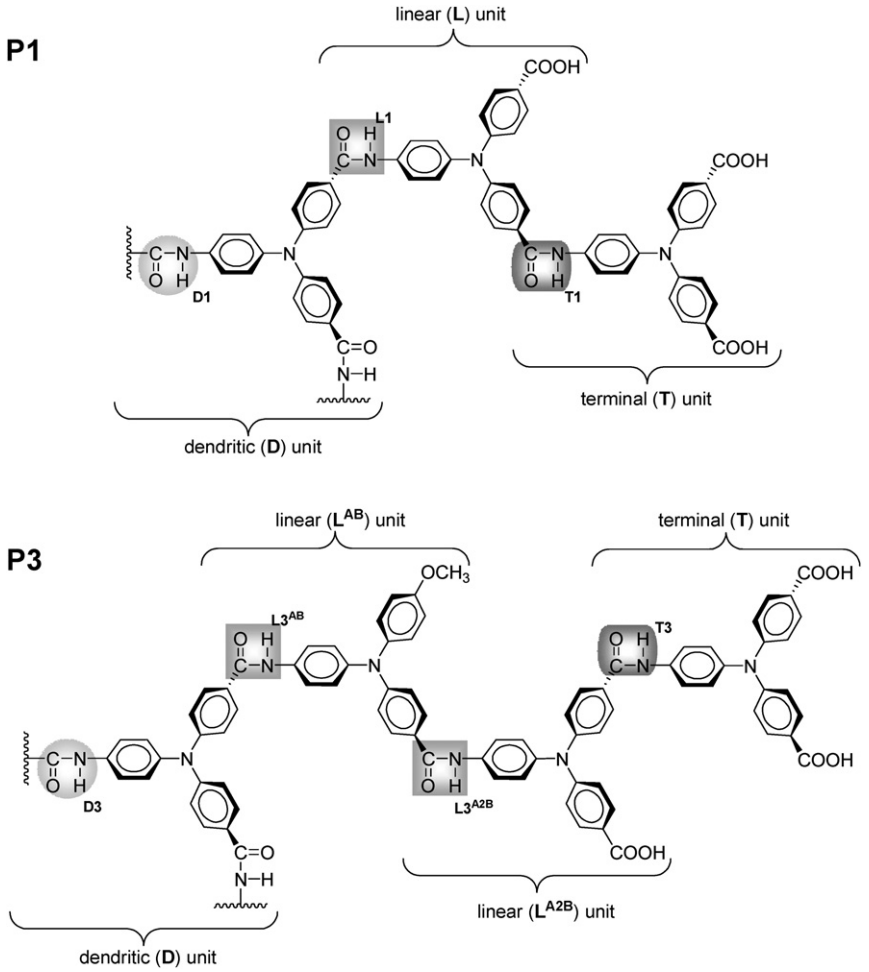

Scheme 3 Possible structural units of the hyperbranched polyamides.

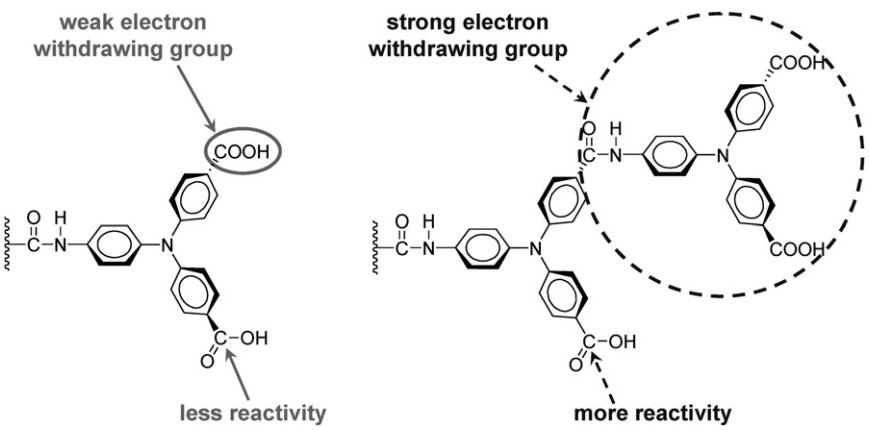

Scheme 4 Terminal (left) and linear (right) units of the hyperbranched polyamides.

these polyamides. The softening temperatures (T_s) (may be referred to as apparent T_g) of the polymer film samples were determined by the TMA method with a loaded penetration probe. They were obtained from the onset temperature of the probe displacement on the TMA traces. In most cases, the T_s values obtained by TMA are comparable to the T_g values measured by the DSC experiments.

Optical properties and electrochemical properties

The optical properties of the hyperbranched polyamides **P1–P3** were investigated by UV-vis and photoluminescence (PL) spectroscopy. The results are summarized in Table S2.† These soluble polymers **P1–P3** exhibited maximum UV-vis absorption bands at 358–363 nm (in THF solution; conc.: 10^{-5} mol/L) and 361–365 nm

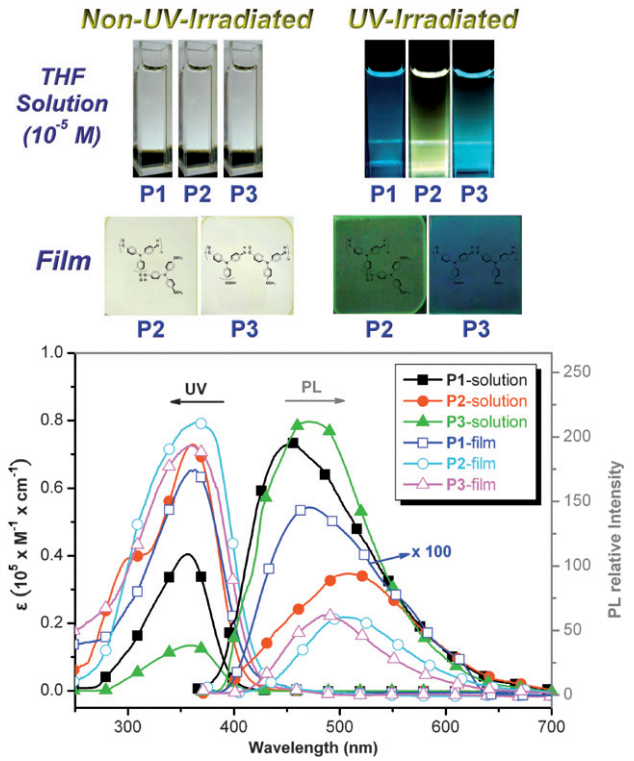

Fig. 2 UV-vis absorptions and PL spectra of **P1–P3** in film and solution (10^{-5} M in THF) states.

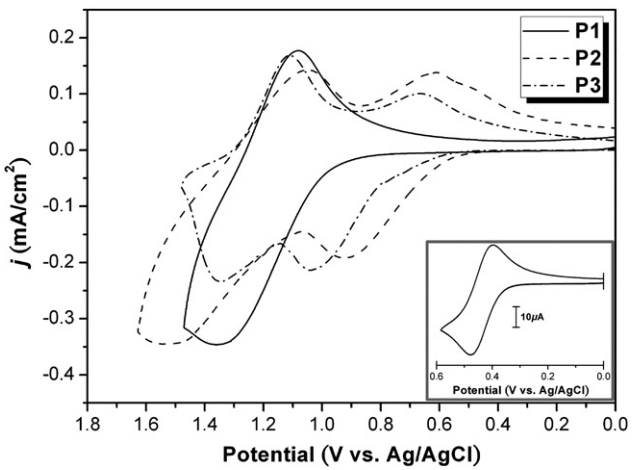

Fig. 3 Cyclic voltammetric diagrams of polyamide **P1–P3** films on an ITO-coated glass substrate and ferrocene (inset) in 0.1 M TBAP/CH_3CN at a scan rate of 50 mV s^{-1}.

(in film state) due to the π–π* transitions resulting from the conjugation between the aromatic rings and nitrogen atom. Fig. 2 shows UV-vis absorption and PL behavior of polyamides **P1–P3** in THF solution and thin film states. The polyamide **P1** exhibited blue PL emission maximum at 455 nm in THF solution with quantum yield of 4.0% referenced by 9,10-diphenylanthracene ($\Phi_F = 0.90$).[20] As shown in Table S2,† the red shift PL emission of **P2** (505 nm) could be attributed to the incorporation of end-capped **B-OMe$_2$** groups, resulting a more extended conjugation length. The cutoff wavelengths (absorption edge; λ_0) from the UV-vis transmittance spectra showed light-color and high optical transparency with cutoff wavelength in the range of 420–423 nm. (Fig. S7).†

The electrochemical properties of the hyperbranched polyamides were investigated by cyclic voltammetry (CV) conducted for the cast film on an indium–tin oxide (ITO)-coated glass slide as working electrode in anhydrous acetonitrile (CH_3CN), using 0.1 M of tetrabutylammonium perchlorate (TBAP) as a supporting electrolyte under a nitrogen atmosphere. The typical CV for polyamides **P1–P3** are shown in Fig. 3 and exhibited a reversible oxidation redox peak for **P1** at the half-wave potential ($E_{1/2}$) around 1.23 V. There are additional redox peaks for **P2** ($E_{1/2} = 0.78$) and **P3** ($E_{1/2} = 0.85$) due to the end-capped **B-OMe$_2$** unit and **AB-OMe** comonomer, respectively. During the electrochemical oxidation scanning of the polyamide **P2** thin films, color of the film changed from colorless to green and then to deep purple. Because of the high electrochemical stability and good adhesion between the polyamide thin film and ITO substrate, polyamide **P2** exhibited reversible CV behavior by continuous 1000 cyclic scans within the first oxidation stage (Fig. S8).† The oxidation potentials of these polyamides as well as their highest occupied molecular orbital (HOMO) and lowest unoccupied molecular orbital (LUMO) are summarized in Table 2. The HOMO level of polyamides **P1–P3** could be estimated from the onset of their oxidation in CV experiments as 5.03–5.44 eV (on the basis that ferrocene/ferrocenium is 4.8 eV below the vacuum level with $E_{onset} = 0.36$ V).

Spectroelectrochemical and electrochromic properties

Spectroelectrochemical investigation was used to evaluate the optical properties of the electrochromic materials, and the polyamide film was cast on an ITO-coated glass slide and a homemade electrochemical cell was built from a commercial ultraviolet (UV)-visible cuvette. The cell was placed in the optical path of the sample light beam in a UV-vis-NIR spectrophotometer to acquire electronic absorption spectra under potential

Table 2 Electrochemical properties of polyamides

	Oxidation[a]					
Polymer	E_{onset}	$E_{1/2(ox1)}$	$E_{1/2(ox2)}$	E_g[b]/eV	HOMO[c]	LUMO
P1	1.00	1.23	—	2.95	5.44	2.49
P2	0.59	0.78	1.24	2.93	5.03	2.10
P3	0.74	0.85	1.23	2.93	5.18	2.25

[a] From cyclic votammograms *versus* Ag/AgCl in CH_3CN. $E_{1/2}$: average potential of the redox couple peaks. [b] The data were calculated from polymer films by the equation: $E_g = 1240/\lambda_{onset}$ (energy gap between HOMO and LUMO). [c] The HOMO energy levels were calculated from cyclic voltammetry and were referenced to ferrocene (4.8 eV; onset = 0.36 V).

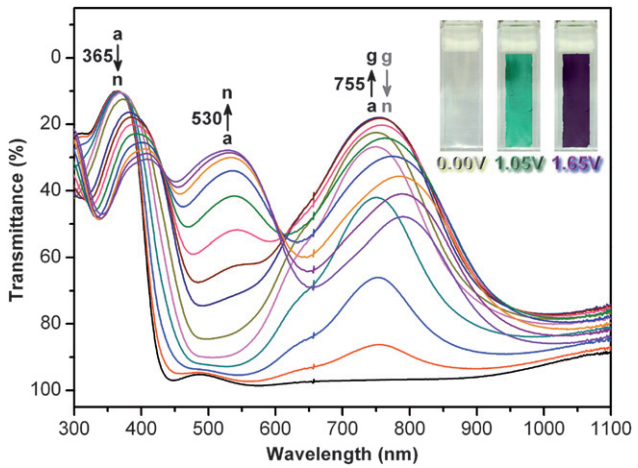

Fig. 4 Electrochromic behavior of polyamide **P2** thin film (~160 nm in thickness) on the ITO-coated glass substrate in 0.1 M TBAP/CH_3CN at applied potentials of (a) 0, (b) 0.60, (c) 0.70, (d) 0.80, (e) 0.90, (f) 1.00, (g) 1.05, (h) 1.15, (i) 1.25, (j) 1.35, (k) 1.45, (l) 1.55, (m) 1.60, (n) 1.65 (V *vs.* Ag/AgCl).

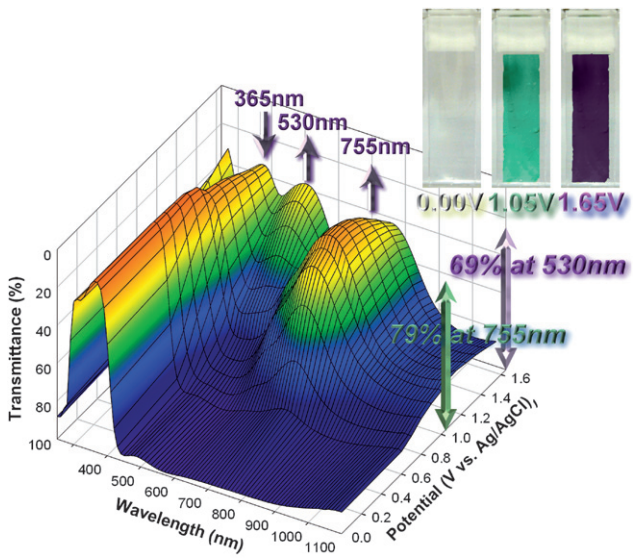

Fig. 5 3-D spectroelectrochemical behavior of the **P2** thin film on the ITO-coated glass substrate in 0.1 M TBAP/CH_3CN from 0 to 1.65 V (*vs.* Ag/AgCl).

control in a 0.1 M TBAP/MeCN solution. The UV-vis-NIR absorbance curves of **P2** film correlated to applied potentials are depicted in Fig. 4, and the three-dimensional transmittance-wavelength-applied potential correlation of this sample is revealed in Fig. 5. The **P2** film exhibited strong absorption at around 365 nm, characteristic of the TPA unit in the neutral form (0 V), being almost colorless and transparent in the visible region. Upon oxidation (increasing applied voltage from 0 to 1.05 V), the intensity of the absorption peak at 365 nm gradually decreased while a new peak at 755 nm gradually increased in intensity due to the formation of a stable cation radical $\mathbf{P2}^{+\bullet}$. As the anodic potential increased to 1.65 V, an additional new absorption band centered at around 530 nm corresponding to another cation radical of **P2** increased gradually. From the inset shown in Fig. 4, the polyamide **P2** film switches from transparent neutral state (colorless; Y: 85; *x*, 0.313; *y*, 0.332) to a highly absorbing semi-oxidized state (green; Y: 40; *x*, 0.266; *y*, 0.406) and a fully oxidized state (deep purple; Y; 2; *x*, 0.244; *y*, 0.112). The distribution of coloration across the polymer film was very homogeneous and still stable even after more than hundreds of redox cycles. The polymer **P2** also shows good contrast in the visible region with an extremely high optical transmittance change ($\Delta\%T$) of 79% at 755 nm for green coloring and 69% at 530 nm for deep purple coloring, respectively.

For electrochromic switching studies, polymer films were cast on ITO-coated glass slides in the same manner as described above, and chronoamperometric and absorbance measurements were performed. While the films were switched, the absorbance at the given wavelength was monitored as a function of time by UV-vis-NIR spectroscopy. The switching time of polyamide **P2** shown in Fig. S9† was calculated at 90% of the full switch because it is difficult to perceive any further color change with the naked eye beyond this point. As depicted in Fig. S9(a),† **P2** thin film revealed switching time of 2.12 s at 0.90 V for the coloring process at 755 nm and 1.21 s for bleaching. The amounts of Q were calculated by integration of the current density and time obtained from Fig. S9(b)† as 1.724 and 1.662 mC cm^{-2} for an oxidation and reduction process at the first oxidation stage, respectively. The ratio of the charge density was 96.4%, indicated that charge injection/extraction was reversible during the electrochemical reactions. The electrochromic stability of the polyamide **P2** film was determined by measuring the optical change as a function of the number of switching cycles shown in Fig. 6. The electrochromic CE ($\eta = \delta OD/Q$) at different switching steps are summarized in Table 3.[21] The electrochromic behavior of **P2** film exhibited high CE up to 426 cm^2/C at 755 nm within 2% of CE loss after switching 100 times between 0 and 0.90 V, and retained 96% of their electroactivity even after further 1000 switching cycles. Considering the oxidation potentials and electrochromic stability, the novel hyperbranched polyamide showed the comparable coloration efficiency with other anodic electrochromic polymers.[18]

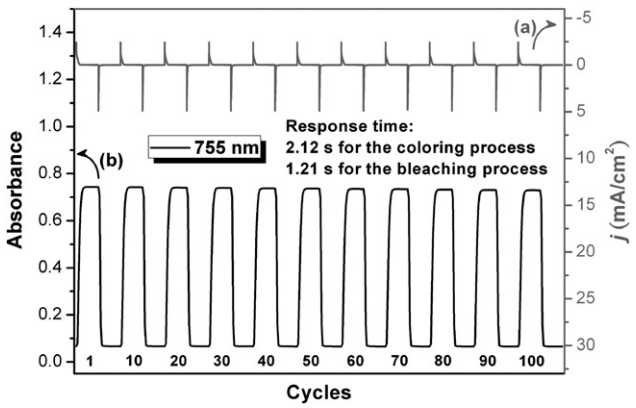

Fig. 6 (a) Current consumption and (b) electrochromic switching between 0 and 0.90 V (*vs.* Ag/AgCl) and absorbance change monitored at 750 nm of polyamide **P2** thin film (~160 nm in thickness) on the ITO-coated glass substrate (coated area: 1.6 × 0.5 cm) in 0.1 M TBAP/CH_3CN with a cycle time of 20 s.

Table 3 Optical and electrochemical data collected for coloration efficiency measurements of polyamide **P2**

Cycling times[a]	δOD_{755}[b]	Q[c]/mC cm^{-2}	η[d]/cm^2/C	Decay[e]/%
1	0.734	1.724	426	0
10	0.733	1.724	425	0.23
20	0.731	1.724	424	0.47
30	0.730	1.724	423	0.70
40	0.728	1.723	423	0.70
50	0.727	1.723	422	0.94
60	0.726	1.723	421	1.17
70	0.725	1.722	421	1.17
80	0.723	1.721	420	1.41
90	0.721	1.721	419	1.64
100	0.720	1.721	418	1.88

[a] Switching between 0.00 and 0.90 (V *vs.* Ag/AgCl). [b] Optical density change at 755 nm. [c] Ejected charge, determined from the *in situ* experiments. [d] Coloration efficiency is derived from the equation: $\eta = \delta OD_{755}/Q$. [e] Decay of coloration efficiency after cyclic scans.

Conclusion

A series of novel electroactive TPA-based hyperbranched aromatic polyamides were readily prepared from the phosphorylation polyamidation reaction of the newly synthesized A_2B monomer, 4-amino-4′,4″-dicarboxytiphenylamine, with AB monomer and end-capping agent, respectively. Because of the TPA-based hyperbranched structure, these polyamides showed good solubility and high thermal stability. In addition, the obtained polymers also revealed valuable electrochromic characteristics such as high contrast in the visible region, high coloration efficiency, and high-level electrochromic/electroactive reversibility.

Acknowledgements

The authors are grateful to the National Science Council of the Republic of China for financial support of this work.

References

1 (*a*) G. R. Newkome, C. N. Moorefield and F. Vogtle, *Dendritic Molecules: Concepts, Syntheses, Perspectives*, VCH: New York, 1996; (*b*) M. Jikei and M. A. Kakimoto, *Prog. Polym. Sci.*, 2001, **26**, 1233; (*c*) M. Scholl, Z. Kadlecova and H. A. Klok, *Prog. Polym. Sci.*, 2009, **34**, 24; (*d*) H. Gao and K. Matyjaszewski, *Prog. Polym. Sci.*, 2009, **34**, 317; (*e*) L. Crespo, G. Sanclimens, M. Pons, E. Giralt, M. Royo and F. Albericio, *Chem. Rev.*, 2005, **105**, 1663; (*f*) S. Tanaka, T. Iso, J. Sugiyama, K. Takeuchi and M. Ueda, *Synth. Met.*, 2005, **154**, 125.

2 (*a*) C. Gao and D. Yan, *Prog. Polym. Sci.*, 2004, **29**, 183; (*b*) B. Voit, *J. Polym. Sci., Part A: Polym. Chem.*, 2005, **43**, 2679; (*c*) C. R. Yates and W. Hayes, *Eur. Polym. J.*, 2004, **40**, 1257.

3 (*a*) C. J. Hawker, R. Lee and J. M. J. Frechet, *J. Am. Chem. Soc.*, 1991, **113**, 4583; (*b*) Z. Shi, Y. Zhou and D. Yan, *Macromol. Rapid Commun.*, 2008, **29**, 412.

4 (*a*) X. Chen, Y. Zhang, B. Liu, J. Zhang, H. Wang, W. Zhang, Q. Chen, S. Peic and Z. Jiang, *J. Mater. Chem.*, 2008, **18**, 5019; (*b*) Z. Jia, H. Chen, X. Zhu and D. Yan, *J. Am. Chem. Soc.*, 2006, **128**, 8144.

5 L. Zhi and K. Müllen, *J. Mater. Chem.*, 2008, **18**, 1472.

6 D. H. Wang, P. Mirau, B. Li, C. Y. Li, J. B. Baek and L. S. Tan, *Chem. Mater.*, 2008, **20**, 1502.

7 K. L. Wang, S. T. Huang, L. G. Hsieh and G. S. Huang, *Polymer*, 2008, **49**, 4087.

8 (*a*) P. Taranekar, Q. Qiao, H. Jiang, I. Ghiviriga, K. S. Schanze and J. R. Reynolds, *J. Am. Chem. Soc.*, 2007, **129**, 8958; (*b*) F. Zhang, Y. H. Luo, J. S. Song, X. Z. Guo, W. L. Liu, C. P. Ma, Y. Huang, M. F. Ge, Z. Bo and Q. B. Meng, *Dyes Pigm.*, 2009, **81**, 224; (*c*) J. Song, F. Zhang, C. Li, W. Liu, B. Li, Y. Huang and Z. Bo, *J. Phys. Chem. C*, 2009, **113**, 13391.

9 (*a*) M. Jikei, R. Mori, S. Kawauchi, M. Kakimoto and Y. Taniguchi, *Polym. J.*, 2002, **34**, 550; (*b*) Q. He, H. Huang, J. Yang, H. Lin and F. Bai, *J. Mater. Chem.*, 2003, **13**, 1085; (*c*) B. Li, X. Xu, M. Sun, Y. Fu, G. Yu, Y. Liu and Z. Bo, *Macromolecules*, 2006, **39**, 456; (*d*) R. Zheng, M. Ha1ussler, H. Dong, J. W. Y. Lam and B. Z. Tang, *Macromolecules*, 2006, **39**, 7973; (*e*) R. H. Lee, W. S. Chen and Y. Y. Wang, *Thin Solid Films*, 2009, **517**, 5747.

10 (*a*) S. Tanaka, T. Iso and Y. Doke, *Chem. Commun.*, 1997, 2063; (*b*) F. Wang, M. S. Wilson, R. D. Rauh, P. Schottland, B. C. Thompson and J. R. Reynolds, *Macromolecules*, 2000, **33**, 2083.

11 (*a*) M. Irie, *Chem. Rev.*, 2000, **100**, 1685; (*b*) *Molecular Switches*, ed. B. L. Feringa, Wiley-VCH, Weinheim, 2001; (*c*) V. Balzani, A. Credi and M. Venturi, *Molecular Devices and Machines: A Journey into the Nano World*, Wiley-VCH, Weinheim, 2003; (*d*) H. Tian and S. J. Yang, *Chem. Soc. Rev.*, 2004, **33**, 85; (*e*) K. D. Belfield, M. V. Bondar, C. C. Corredor, F. E. Hernandez, O. V. Przhonska and S. Yao, *ChemPhysChem*, 2006, **7**, 2514; (*f*) H. Tian and Y. Feng, *J. Mater. Chem.*, 2008, **18**, 1617.

12 (*a*) P. M. S. Monk, R. J. Mortimer and D. R. Rosseinsky, *Electrochromism: Fundamentals and Applications*; VCH: Weinheim, Germany, 1995; (*b*) D. R. Rosseinsky and R. J. Mortimer, *Adv. Mater.*, 2001, **13**, 783; (*c*) P. R. Somani and S. Radhakrishnan, *Mater. Chem. Phys.*, 2003, **77**, 117; (*d*) T. Zhang, S. Liu, D. G. Kurth and C. F. J. Faul, *Adv. Funct. Mater.*, 2009, **19**, 642; (*e*) A. Maier, A. R. Rabindranath and B. Tieke, *Adv. Mater.*, 2009, **21**, 959.

13 (*a*) N. Yamazaki, F. Higashi and J. Kawabata, *J. Polym. Sci. Polym. Chem. Ed.*, 1974, **12**, 2149; (*b*) N. Yamazaki, M. Matsumoto and F. Higashi, *J Polym. Sci. Polym. Chem. Ed.*, 1975, **13**, 1373.

14 (*a*) P. E. Cassidy, *Thermally Stable Polymers*, Marcel Dekker: New York, 1980; (*b*) H. H. Yang, *Aromatic High-Strength Fibers*, Wiley: New York, 1989.

15 M. Jikei and M. A. Kakimoto, *J. Polym. Sci. Part A: Polym. Chem.*, 2004, **42**, 1293.

16 P. J. Flory, *J. Am. Chem. Soc.*, 1952, **74**, 2718.

17 (*a*) H. R. Kricheldorf and T. Stukenbrock, *J. Polym. Sci. Part A: Polym. Chem.*, 1998, **36**, 2347; (*b*) J. Li and Z. Bo, *Macromolecules*, 2004, **37**, 2013; (*c*) M. Sun, J. Li, B. Li, Y. Fu and Z. Bo, *Macromolecules*, 2008, **38**, 2651.

18 (*a*) C. W. Chang, G. S. Liou and S. H. Hsiao, *J. Mater. Chem.*, 2007, **17**, 1007; (*b*) G. S. Liou and C. W. Chang, *Macromolecules*, 2008, **41**, 1667; (*c*) C. W. Chang and G. S. Liou, *J. Mater. Chem.*, 2008, **18**, 5638; (*d*) C. W. Chang, H. J. Yen, K. Y. Huang, J. M. Yeh and G. S. Liou, *J. Polym. Sci. Part A: Polym. Chem.*, 2008, **46**, 7937.

19 G. S. Liou and K. H. Lin, *J. Polym. Sci. Part A: Polym. Chem.*, 2009, **47**, 1988.

20 H. J. Yen and G. S. Liou, *J. Polym. Sci. Part A: Polym.Chem.*, 2008, **46**, 7354.

21 H. J. Yen and G. S. Liou, *Chem. Mater.*, 2009, DOI: 10.1021/cm9015222.